Chin. Geogra. Sci. 2010 20(6) 513–521
DOI: 10.1007/s11769-010-0423-3

Modeling All-sky Global Solar Radiation Using MODIS Atmospheric Products: A Case Study in Qinghai-Tibet Plateau

ZHANG Hailong, LIU Gaohuan, HUANG Chong
(*State Key Laboratory of Resources and Environmental Information System, Institute of Geographic Sciences and Natural Resources Research, Chinese Academy of Sciences, Beijing 100101, China*)

Abstract: The surface solar radiation (SSR) is of great importance to bio-chemical cycle and life activities. However, it is impossible to observe SSR directly over large areas especially for rugged surfaces such as the Qinghai-Tibet Plateau. This paper presented an improved parameterized model for predicting all-sky global solar radiation on rugged surfaces using Moderate Resolution Imaging Spectroradiometer (MODIS) atmospheric products and Digital Elevation Model (DEM). The global solar radiation was validated using 11 observations within the plateau. The correlation coefficients of daily data vary between 0.67–0.86, while those of the averages of 10-day data are between 0.79–0.97. The model indicates that the attenuation of SSR is mainly caused by cloud under cloudy sky, and terrain is an important factor influencing SSR over rugged surfaces under clear sky. A positive relationship can also be inferred between the SSR and slope. Compared with horizontal surfaces, the south-facing slope receives more radiation, followed by the west- and east-facing slopes with less SSR, and the SSR of the north-facing slope is the least.
Keywords: DEM; all sky; surface solar radiation; MODIS; Qinghai-Tibet Plateau

1 Introduction

Surface solar radiation (SSR) is the principal energy source for physical, biological and chemical processes, such as snow melt, plant photosynthesis, evaporation and crop growth, and is also a variable needed for biophysical models, hydrological simulation models and mathematical models of natural processes at local, regional and global scales (Gueymard, 2003a). In the world, there are a large number of measuring basic meteorological variables, but few stations measuring solar radiation because of not being able to afford the measuring equipments and techniques involved, especially in highlands and mountainous areas. In locations where radiation measurements are sparse, theoretical simulation based on basic meteorological data and remote sensing data is an effective way to estimate the available solar radiation.

In general, three types of methods can be used to estimate solar radiation on the ground. The first type, the spectral transfer method, takes into account the vertical atmospheric in-homogeneity through a series of superimposed scattering and absorbing layers, including LOWTRAN and MODTRAN. The second one is the empirical model with a representative of A-P (Ångström-Proscott) model using the linear or non-linear regression equations between the observed radiation and meteorological variables such as sunshine hours (Ertekin and Evrendilek, 2007), air temperature (Winslow *et al*., 2001), precipitation (Liu and Scott, 2001), relative humidity and cloudiness (Mubiru *et al*., 2007). The third one, the parametric model, is based on the same physical principles as the spectral transfer method, and str0 ongly simplifies estimation procedures with a set of parameterizations, which is dependent on preliminary integration of spectral transmittance functions and sensitive to the most important extinction sources of the atmosphere (Wang *et al*., 2006). The third type includes the one-band model which considers the solar spectrum as one layer (Yang *et al*., 2001), such as MLWT (Gueymard, 2003a) and REST (Gueymard, 2003a; 2003b), and the two-band model which divides the whole spec-

Received date: 2010-02-09; accepted date: 2010-06-28
Foundation item: Under the auspices of Knowledge Innovation Programs of the Chinese Academy of Sciences (No. KZCX2-YW-308), National Natural Science Foundation of China (No. 40771172, 40901223)
Corresponding author: ZHANG Hailong. E-mail: zhlnjnu@163.com

trum into the ultraviolet/visible band and the infrared band like CPCR2 (Gueymard, 1989), REST2 (Gueymard, 2008). Due to the complexity of the ground and the great variation of the weather conditions, each kind of the above models has its shortcomings. For most practical purposes and users, the rigorous spectral transfer methods show to be unusable due to the large amount of atmospheric information required or time consuming; the empirical models are usually not easy to be extrapolated to regional or global scales without local calibration because they are dependent on the local climatic conditions, the number and spatial distribution of meteorological stations and terrain undulation; and the parametric models are designed only for clear sky with horizontal surfaces.

The complex terrain and the amount and distribution of solar energy on the Qinghai-Tibet Plateau have significant influences on the Asian monsoon and the global climate changes (Bai and Xu, 2004; Lau *et al*., 2006). However, the atrocious geographical and natural conditions make it quite difficult for the scientists to carry out more and frequent solar radiation observations. Previous researchers focused on the energy budget at typical areas using sparse meteorological observations (Wu *et al*., 2005; Li *et al*., 2007), but they could not map the solar energy over the Qinghai-Tibet Plateau at different spatio-temporal scales. Up to now, however, we still know little about the thermal regime of the land surfaces over the plateau.

Since solar radiation data are scarce in the Qinghai-Tibet Plateau, simply spectral models are inapplicable over large areas. To solve the problem, in this study, a new improved parameterized model for estimating SSR, including direct solar radiation, diffuse solar radiation and global solar radiation, under actual weather and terrain conditions of the Qinghai-Tibet Plateau was proposed by incorporating Moderate Resolution Imaging Spectroradiometer (MODIS) atmospheric products with Digital Elevation Model (DEM). The model was validated by using 11 observations within the plateau, and the errors and the parameter sensitivities were also analyzed.

2 Data and Methodology

2.1 Study area

The study area is a part of the Qinghai-Tibet Plateau within the territory of China, extending from 26º00′12″N to 39º46′50″N and from 73º18′52″E to 104º46′59″E, covering an area of 2.5724×10^6 km^2 (Zhang *et al*., 2002) (Fig. 1). The altitude of the study area is 60–8 790 m above sea level. The eastern and southern parts of the Qinghai-Tibet Plateau are influenced by the south-east monsoon from the Pacific Ocean and the south-west monsoon from the Indian Ocean, respectively (Li and Kang, 2006). Most parts of the plateau belong to the semiarid or arid areas. The annual precipitation varies from 200 mm to 1 600 mm, of which 60%–70% happens in summer. The mean temperature in January and July is 0–13℃ and 8–18℃, respectively. Forests are distributed in the warm and humid southeastern parts and grasslands in the cold and dry central and northwestern parts. Cultivated crops are mainly located in lower altitude with mild climatic conditions between grasslands and forests, while sparse shrubs or bare grounds mostly lie to the north of the grasslands with hostile climate (Xu and Liu, 2007).

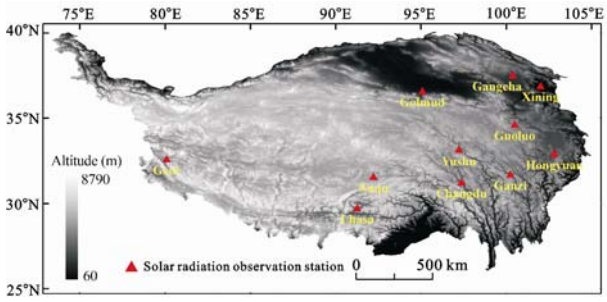

Fig. 1 Location of study area and global solar radiation observation stations

2.2 Data sources

All of the atmospheric parameters required by the proposed method were readily available from LAADS web (Level 1 and Atmosphere Archive and Distribution System) (http://ladsweb.nascom.nasa.gov/data/). The geolocation data and sensor viewing geometry were taken from the geolocation product MOD03/MYD03. The total atmospheric water content was acquired from MOD05/MYD05. The most sensitive parameters, cloud optical thickness and cloud fraction, were available at a resolution of 1 km from MOD06/MYD06. The snow albedo parameter was acquired from MOD10 products. DEM data with 30 m spatial resolution was acquired from the international scientific data service platform

(http://srtm.datamirror.csdb.cn/search1.jsp). Observations of SSR from National Meteorological Information Center, China Meteorological Administration were also used to evaluate the model. All MODIS daily data and observations were collected in 2007.

All spatial data were collected in 2007 and georeferenced to geographic coordinate system with a spatial resolution of 1 km. The MODIS Terra observation was assumed to be representative of the early morning atmospheric conditions, while the MODIS Aqua observation was used for the late afternoon conditions. The atmospheric conditions during the crucial midday part, when irradiance is the highest, was linearly interpolated from the corresponding atmospheric products of the two observations. When either of the two observations did not report any of the least sensitive parameters (cloud optical thickness or total atmospheric water content), these values were held constant for the day from the other observation. If the parameters were missing from both observations then no calculation was made.

2.3 Model description

The amount of global solar radiation received by a given surface is a function of the solar declination, atmospheric transmittance, geographical location, sun elevation angle, surface slope, aspect and elevation (Allen *et al*., 2006). Total radiation incident on a tilted plane consists of two components: direct solar radiation and diffuse solar radiation.

2.3.1 Direct solar radiation

Under cloudy sky, the atmosphere is treated as a combination of a cloud layer and a clear layer from the cloud bottom downwards. The solar irradiance is attenuated by absorption and reflection of the cloud in the top layer under cloudy sky, and the main extinction processes in the clear layer are: aerosol extinction, Rayleigh scattering, and absorption by ozone, uniformly mixed gases and water vapor.

The direct solar irradiance under cloudy sky can be calculated by incorporating the transmittance of cloud layer and clear sky (Gueymard, 2008).

$$I_{\mathrm{dir}i} = I_{0i} T_{\mathrm{clo}i} T_{\mathrm{cle}i} E_0 \sin h_{\alpha\beta} \quad (1)$$

where $I_{\mathrm{dir}i}$ denotes the direct solar irradiance at the ith band on tilted surface, i = 1, 2, i.e., ultraviolet/visible band (0.29–0.70 μm) and near infrared band (0.70–4.00 μm), respectively; I_{0i}, the solar constant at the ith band with the values I_{01} = 0.038 MJ/(m^2 · min) and I_{02} = 0.043 MJ/(m^2 · min) (Gueymard, 1989); $T_{\mathrm{clo}i}$ and $T_{\mathrm{cle}i}$ represent the transmittances of the cloud layer and the clear layer at the ith band, respectively; E_0, sun-earth distance correction factor; $h_{\alpha\beta}$ refers to the sun height angle of a slope with an aspect α (radian) and a slope β (radian), which is calculated using the algorithm provided by Wang *et al*. (2006) .

The transmittances for clear sky and cloudy sky are calculated using equations (2), (3) and (4):

$$T_{\mathrm{cle}i} = T_{\mathrm{O}i} T_{\mathrm{R}i} T_{\mathrm{G}i} T_{\mathrm{W}i} T_{\mathrm{A}i} \quad (2)$$

where $T_{\mathrm{O}i}$, $T_{\mathrm{R}i}$, $T_{\mathrm{G}i}$, $T_{\mathrm{W}i}$ and $T_{\mathrm{A}i}$ represent the transmittance functions for ozone absorption, Rayleigh scattering, uniformly mixed gases absorption, water vapor absorption and aerosol extinction at the ith band, respectively. The transmittance for clear sky is acquired using the algorithm provided by Gueymard (1989; 2008).

$$T_{\mathrm{clo1}} = 1 - (\gamma(\mu_0)\tau_C / \mu_0) / (1 + \gamma(\mu_0)\tau_C / \mu_0) \quad (3)$$

$$T_{\mathrm{clo2}} = 4U / V \quad (4)$$

where μ_0 is solar zenith angel (radian); $\gamma(\mu_0)$ is the back scattered fraction of incident radiation as a function of μ_0; τ_C is the cloud optical thickness, which can be derived from MODIS atmospheric products (MOD06/MYD06); U and V are parameters dependent on $\gamma(\mu_0)$ and μ_0. Values for $\gamma(\mu_0)$, U and V are linearly interpolated from the look-up table given in Stephens (1978) and Stephens *et al*. (1984).

Daily direct solar radiation (W_{dir}) can be calculated by integrating the irradiance from sunrise to sunset in 30 min intervals using Equation (5).

$$W_{\mathrm{dir}} = \sum_{t=1}^{n} \left(\int_{\omega sr}^{\omega ss} (I_{\mathrm{dir1}} + I_{\mathrm{dir2}}) \mathrm{d}t \times f(dem) \right) \quad (5)$$

where ωsr and ωss (radian) are the solar hour angles at sunrise and sunset respectively during the time intervals; $f(dem)$ is the shading status of a object depending on the status of at sunrise and sunset during the time intervals. If the object were both shaded at sunrise and sunset, it was assigned 0, otherwise it was assigned 1, and it was assigned 0.5 while the status was opposite at sunrise and sunset.

Due to oblique viewing angles of MODIS sensors, the apparent position of cloud as seen from the satellite will be off its projected location, which is called three dimensional (3D) effects. At oblique sun angles, the cloud

shadow becomes displaced from the projected cloud position. The true location of the cloud shadow at any given time is corrected by taking a single cloud top height for each pixel and projecting this height to the surface for the given viewing geometry or solar elevation angle. As the cloud top height is difficult to retrieve and a rough estimation of the cloud top height can be used without taking much considerable bias (Wyser *et al*., 2002). In this paper, the cloud top height is held a constant of 5 km.

2.3.2 Diffuse solar radiation

Diffuse solar irradiance ($I_{\mathrm{dif}i}$) at ground level is treated as a combination of three individual components, i.e., sky diffuse irradiance (I_{si}) (corresponding to Rayleigh diffuse irradiance ($I_{\mathrm{R}i}$), aerosol diffuse irradiance ($I_{\mathrm{A}i}$)), multiple backscattering between surface and sky ($I_{\mathrm{ss}i}$), and the additional irradiance from the neighborhood ($I_{\mathrm{n}i}$) for tilted surfaces.

The total cloud fraction (TCF) is one of the effective factors that reflect the impact of cloud on solar irradiance. Equation (6) is used to consider the cloud impact on diffuse solar irradiance:

$$I_{\mathrm{dif}i} = (I_{si} + I_{\mathrm{ss}i} + I_{\mathrm{n}i}) \times (1 - TCF) + (1 - T_{\mathrm{clo}i}) \times TCF \times (I_{\mathrm{dir}i} + I_{si} + I_{\mathrm{ss}i} + I_{\mathrm{n}i}) \quad (6)$$

$$I_{si} = (I_{\mathrm{R}i} + I_{\mathrm{A}i}) \times V \times (1 + \cos\alpha) \quad (7)$$

$$I_{\mathrm{ss}i} = I_{\mathrm{ss}i(\mathrm{hor})} \times V \times (1+\cos\alpha) \quad (8)$$

$$I_{\mathrm{n}i} = \rho_{\mathrm{g}i}(I_{si} + I_{\mathrm{ss}i} + I_{\mathrm{dir}i(\mathrm{hor})}) \times (1 + \cos\alpha - V) / 2 \quad (9)$$

where TCF (%) is derived from MODIS atmospheric products; V is terrain openness factor; $I_{\mathrm{ss}i(\mathrm{hor})}$ is multiple backscattering, between surface and sky on horizontal surface (MJ/(m^2·min)); $\rho_{\mathrm{g}i}$ is the ground albedo of the ith band derived from MOD10 product; $I_{\mathrm{dir}i(\mathrm{hor})}$ is the direct solar irradiance at the ith band on horizontal surface.

Daily diffuse solar radiation (W_{dif}) can be calculated by integrating the irradiance from sunrise to sunset in 30 min intervals using Equation (10).

$$W_{\mathrm{dif}} = \sum_{t=1}^{n} \left(\int_{wsr}^{wss} (I_{\mathrm{dif1}} + I_{\mathrm{dif2}}) \mathrm{d}t \right) \quad (10)$$

3 Results and Analyses

3.1 Model validation

The improved parameterized model presented in this paper was validated using observations from 11 stations within the Qinghai-Tibet Plateau (Fig. 1). Model validation was made by means of mean bias error (*MBE*) and correlation coefficient (R^2). As the components of solar radiation (direct radiation and diffuse radiation) were only observed in Lhasa and Golmud stations, they were validated using the observations of the two stations, while the global solar radiation were validated using 11 observations. The scatter plots of the simulated and observed direct and diffuse radiation are shown in Fig. 2, and the global radiation results are shown in Table 1.

From Fig. 2 it can be seen that the correlation coefficients between the simulated solar radiation and the observed series were around 0.70 except the direct radiation of Golmud with 0.82. The *MBE*s were –0.46 MJ/(m^2·d) (Lhasa) and 0.68 MJ/(m^2·d) (Golmud) for direct radiation, and 0.03 MJ/(m^2·d) (Lhasa) and 0.26 MJ/(m^2·d) (Golmud) for diffuse radiation, respectively. Table 2 shows that the correlation coefficients of simulated daily and 10-day average of global solar radiation were higher than 0.71 and 0.85, respectively, except for Guoluo with R^2 of 0.67 and 0.79. It can be inferred that the proposed model can yield a better performance to simulate daily SSR compared with the sunshine based model proposed by Shen (1987).

3.2 Error analysis

(1) Error from different spatial resolutions of the observed and simulated data. Considering the spatial resolution, the data could only be measured at the point where the global radiation meter is located. However, the simulated global radiation has the spatial resolution of 1 km, which may affect the eventual simulating results.

(2) Error from spatio-temporal resolution of data sources. The spatio-temporal resolution of the MODIS atmospheric data is a bit rough for the Qinghai-Tibet Plateau. The variation of cloud could not be described accurately with only two instantaneous images during the daytime. Meanwhile, the weather in the plateau, especially in rainy season, changes frequently. Furthermore, with the spatial resolution of 1 km, much detailed topography information is ignored and the deriving parameters such as slope and aspect will inevitably contain errors.

As the correlation coefficient of daily data varies greatly among the 11 stations, the Golmud and Guoluo station with highest R^2 and lowest R^2 were selected to further analyze the effect of spatial resolution on the model performance, and the variation of extraterrestrial

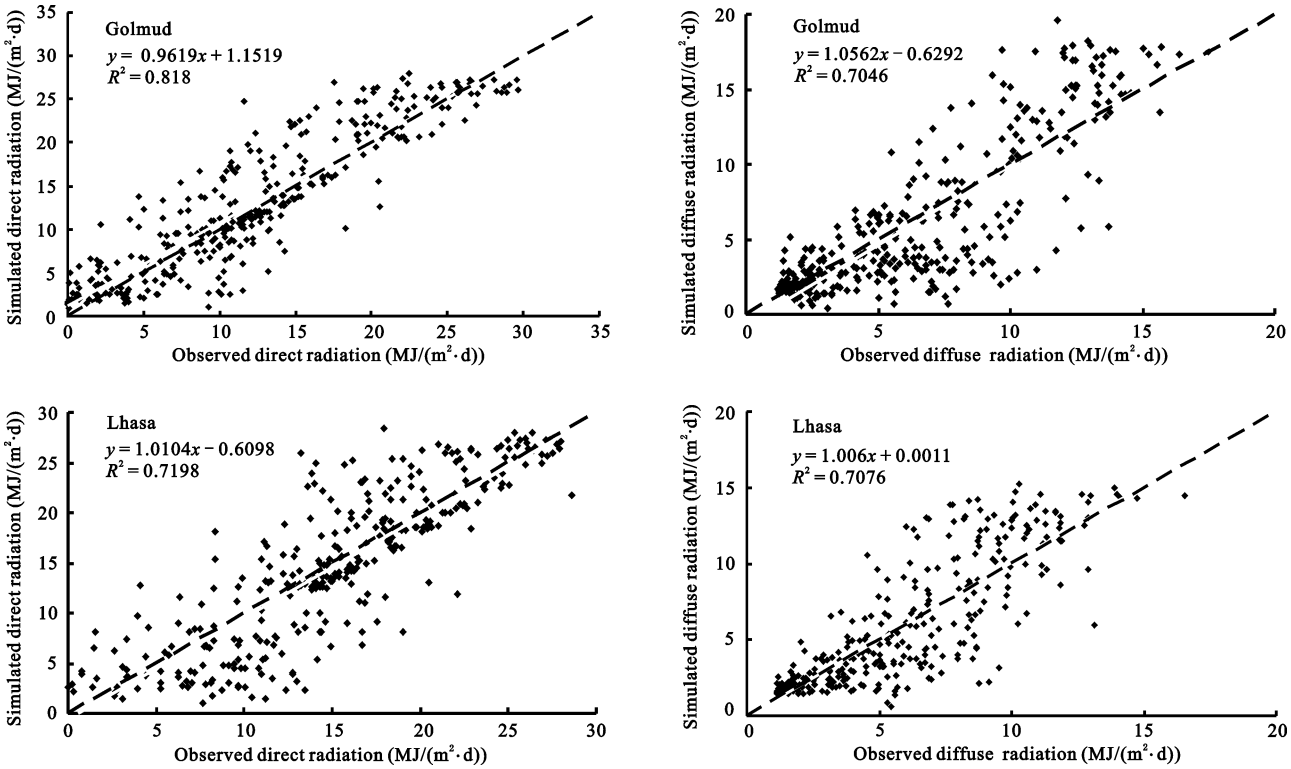

Dash line represents the 1∶1 regression

Fig. 2 Scatter plots of simulated and observed daily solar radiation at Golmud and Lhasa in 2007

Table 1 Accuracy assessment of global solar radiation simulation

	Golmud	Lhasa	Geer	Naqu	Gangcha	Xining	Guoluo	Hongyuan	Ganzi	Yushu	Changdu
MBE	2.25	–2.05	–4.76	–0.97	–1.31	13.98	4.05	2.08	–3.54	–14.25	–0.77
R^2*	0.86	0.77	0.85	0.74	0.75	0.83	0.67	0.72	0.71	0.77	0.71
R^2**	0.95	0.96	0.97	0.88	0.91	0.95	0.79	0.85	0.91	0.97	0.92

Notes: *MBE* represents daily mean bias error; * represents correlation coefficient of daily data; ** represents correlation coefficient of averages of 10-day data

solar radiation (ESR) at a resolution of 30 m and 1 000 m were also computed respectively.

The ESR increased at both sites as the topography caused less obstruction at a coarse resolution of DEM (Fig. 3). The ESR with the resolution of 1 000 m at Guoluo station was lower than that on horizontal surface due to the rouged surfaces, and the daily variation of ESR with 30 m resolution is greater than that with 1 000 m resolution (Fig. 3a). The ESR with the resolution of 1 000 m at Golmud is the same as that on horizontal surface due to the lower terrain (slope = 0.3° at 1 000 m resolution) (Fig. 3b). The mean annual difference of ESR at Guoluo and Golmud at 30 m and 1 000 m resolution are 9.43 MJ/(m^2·d) and 12.79 MJ/(m^2·d), respectively.

The Terra and Aqua satellite platform cross the Equator during the daytime at approximately 10:30 local time on the descending node, and 13:30 local time on the ascending node, respectively. The gap between the weather conditions when MODIS crossed and the weather variation during the daytime may contribute a lot to the model error. As the ground was covered by cloud at Guoluo during most time of 2007 (Fig. 4), the cloud variation can not be described accurately using two instantaneous MODIS image per day, furthermore, the uncertainty of the MODIS products (MOD05/MYD05 and MOD06/MYD06) will arise when the ground was covered by thick cloud and precipitation occurred. The weather of Golmud was clear or partially clear during the year of 2007, the uncertainty of the MODIS products was lower, and thus the model performance was much better. It can be concluded that the

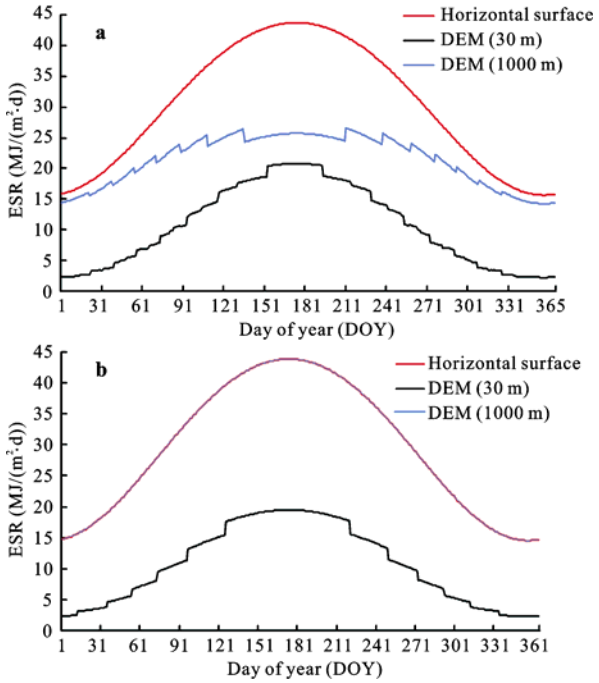

For Guoluo, when resolution is 30 m, slope is 2.2° and aspect is northeast; when resolution is 1000 m, slope is 1.4° and aspect is shouthwest. For Golmud, when resolution is 30 m, slope is 3.7° and aspect is northeast; when resolution is 1000 m, topography is almost horizontal, and curve of Golmud at resolution of 1000 m is overlapped with that on horizontal surface

Fig. 3 Variations of daily extraterrestrial solar radiation (ESR) at Guoluo (a) and Golmud (b)

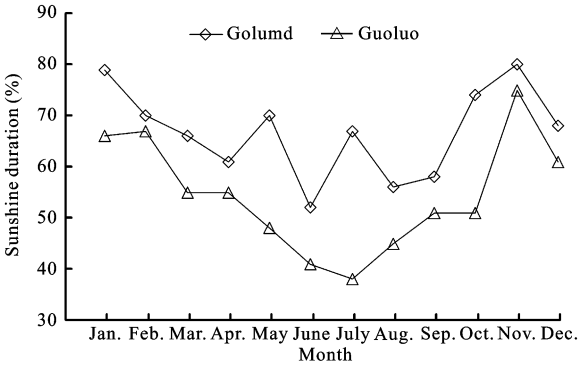

Fig. 4 Monthly sunshine duration at Guoluo and Golmud in 2007

the temporal resolution of the atmospheric parameters was more important than the spatial resolution of the terrain.

(3) Error from data sources themselves. Another possible reason for the biases may be introduced by the MODIS cloud-detection algorithm with a maximum uncertainty of 200% (Houborg *et al*., 2007). As cloud is the main controlling factor of the SSR, large uncertainty of the cloud parameters will bring much bias of the model performance. Besides, the longitude and latitude of the stations acquired from National Meteorological Information Center, China Meteorological Administration are accurate to minute instead of second, which results in a mismatch of one or two kilometers.

3.3 Topographic effects on surface solar radiation

Topographic factors such as slope, aspect and altitude have important effects on incident solar irradiance on uneven land surfaces. An assessment on the degree of the effects should be considered. A variable of R_b is defined to be the ratio of the direct solar radiation on tilted surfaces to that on horizontal surface, and the curves of R_b at the point with a latitude of 22°N in January verse slope and aspect are shown in Fig. 5 (without considering the obstruction of the terrain).

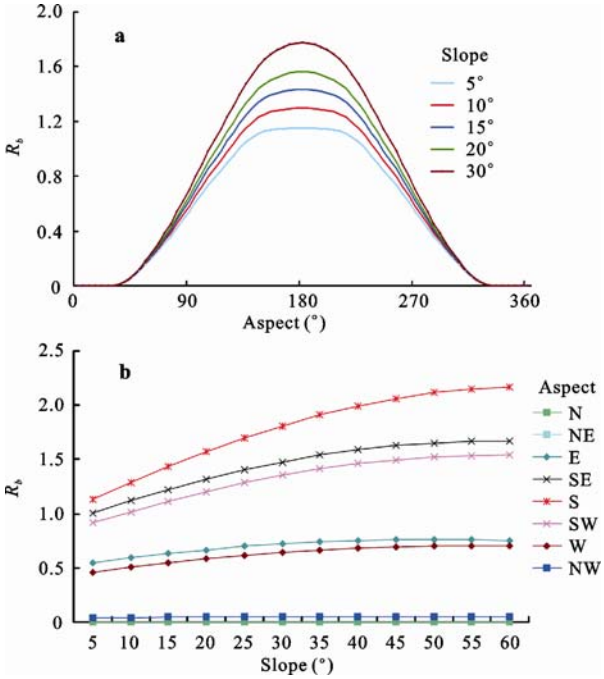

Aspect is defined as north (0°), east (90°), south (180°) and west (270°)

Fig. 5 Ratio of direct solar radiation on tilted surfaces to that on horizontal surface (R_b) verse aspect (a) and slope (b)

More direct solar radiation can be received under a given slope as the aspect changes from north to south, and a positive relationship can be found between the direct solar radiation and the slope, while the aspect was held constant (Fig. 5a). The south-facing slopes can receive more radiation than horizontal surfaces, followed by the east slope and the west slope, while the north-facing slopes receive less radiation than horizontal sur-

faces (Fig. 5b). However, it should be noted that the maximum value of R_b depends on the latitude of the target, the surface roughness and the day of the year.

3.4 Parameter sensitivity analysis

A sensitivity study was carried out to observe the relationship between the surface solar radiation and the surface roughness and cloud. The results show that both of them may play an important role in the transmittance of solar radiation under different weather conditions.

The direct and diffuse radiation had the characteristics of being the strongest in summer (Fig. 6). Under clear sky, the topography is the primary controlling factor of the surface direct solar radiation (Fig. 5, Fig. 6). However, the cloud is the main attenuation of the direct radiation rather than topography for actual weather conditions. Much less diffuse radiation can be received on the tilted surfaces than horizontal surface under clear sky, while cloud is the primary contributor to diffuse radiation instead of the topography under cloudy sky. It can be concluded that as cloud has the strongest impact on shortwave radiation at ground, the spatio-temporal resolution and the accuracy of the cloud dominates the model accuracy.

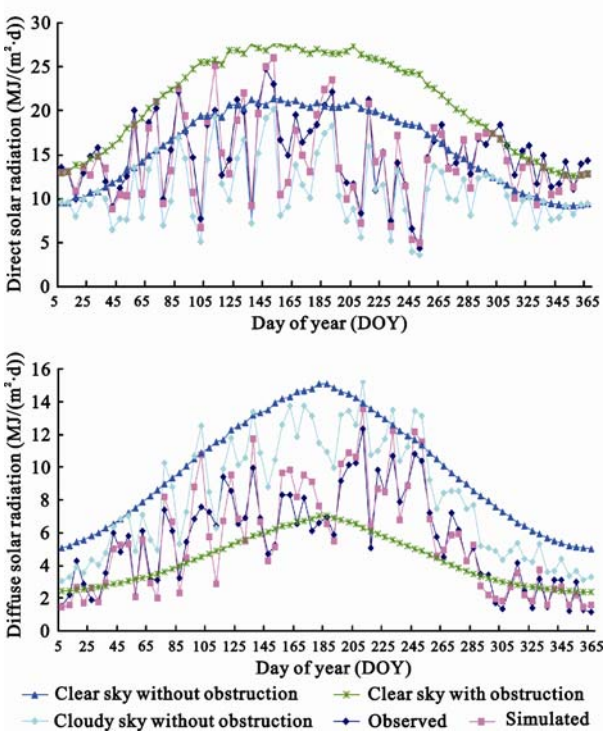

Fig. 6 Daily solar radiation under different conditions at Lhasa station

From contrasting results between the observed and simulated data shown in Fig. 6, it is easily to conclude that the model results will be much better especially for diffuse radiation if the topographic conditions were taken into account.

4 Discussion

The objective of this study was to develop a simplified method for calculating SSR using pairs of MODIS products. The overall accuracy obtained with the method relative to the measured data indicates that the model might be accurate enough to be applied in biophysical models. The model can be extrapolated to other areas without further validation as the inputs were solely from satellite data and the attenuation factors of SSR were also considered.

The errors caused by the aerosol can be neglected in the Qinghai-Tibet Plateau with a relatively low aerosol load. But the effect of the aerosol will be much more pronounced in the SSR estimation of other areas with higher aerosol load, and an accurate input of aerosol data is advised when simulating SSR using the proposed model. The short temporal scale of many atmospheric processes (particularly the cloud parameters in the tropics and mountainous areas) is still one of the problems causing of the model accuracy. Though higher temporal resolution data can be obtained from meteorological satellites, the degration at higher latitude and sensor viewing angle makes it inapplicable in practice. International Satellite Cloud Climatology Project (ISCCP) produces atmospheric parameters including cloud optical thickness at a spatial resolution of 30 km and a temporal resolution of 3 h. In many circumstances, the 30 km spatial resolution introduces generalizations of surface heterogeneity that have a profound effect on irradiance, especially for mountainous regions such as Qinghai-Tibet Plateau. It is a dilemma to choose high temporal resolution at reduced spatial resolution, or high spatial resolution at reduced temporal resolution (Van Laake and Sanchez-Azofeifa, 2004)

A commonly used method in simulating SSR is the sunshine duration based equations, which builds upon empirical relationships, and there is no mechanism to incorporate actual atmospheric conditions. Compared with the Food and Agricultural Organization (FAO) model with MBE of –2.66 MJ/(m^2·d) and –1.05 MJ/(m^2·d) at

Lhasa and Golmud respectively, Gopinathan model (GM) with MBE of –3.32 MJ/(m^2·d) and –0.72 MJ/(m^2·d) at Lhasa and Golmud respectively, and A-P model with MBE of –2.42 MJ/(m^2·d) and –1.13 MJ/(m^2·d) at Lhasa and Golmud respectively (Yang *et al*., 2006), the proposed model in this paper can simulate SSR with comparable accuracy. Further, the above models are completely insensitive to topography and it would be difficult to extrapolate the results over large area. As Zelenka *et al*. (1999) indicated, only 25 km away from a ground station, the satellite-derived radiation becomes more accurate than extrapolated ground measurements. The SSR derived from MODIS products performs much better both in spatial and temporal domain.

5 Conclusions

This paper presented an improved parameterized model to calculate direct and diffuse solar radiation on tilted surfaces for all-sky conditions. The inputs to the model are solely from daily pairs of MODIS Terra and Aqua images, and this makes the method particularly suitable for mapping regional SSR from satellite imagery. Compared to field observations, the simulated daily direct and diffuse radiation values have correlation coefficients of 0.70–0.82, daily global surface solar radiation has correlation coefficients of 0.67–0.86, but ten-day averaged values show much better correspondence with observations, yielding average correlation coefficient of around 0.92.

It can be concluded that under clear sky, the topography has great effect on direct and diffuse solar radiation, while cloud is the primary attenuation for solar radiation rather than topography under cloudy sky. The direct radiation has a positive relationship with slope. The accuracy of modeled SSR was improved greatly while the terrain obstruction was taken into account. Under clear sky, the obstruction of the terrain is a main factor of the solar radiation attenuation, while the cloud plays a greater role than terrain under cloudy sky.

With the sensitive parameters, cloud optical thickness and precipitable water, derived from pairs of MODIS images, moderately detailed maps of global shortwave radiation on rugged surface can be produced for regional studies. There are at most two observations of atmospheric conditions per day, which are sufficient to capture the major diurnal atmospheric dynamics in many places on the Earth, but can not describe the higher frequency events such as appearance and clearing of cloud cover accurately. One should rather rely on temporally aggregated data to get a more accurate estimate of solar radiation due to the daily variation of cloud.

While the combination of pairs of images from MODIS Terra and Aqua sensors yields good estimates of surface solar radiation, the use of new generation of meteorological satellites (with the spatial resolution ranges from 1 km to 10 km and temporal resolution ranges from 30 minutes to 12 hours, such as METEOSAT Second Generation, GOES satellite, and GMS satellites) or NCEP/NCAR reanalysis data holds great promise for the accurate estimation of surface solar radiation from remotely sensed imagery.

Acknowledgement

The authors would like to thank Dr. Christian A Gueymard (Solar Consulting Services, P. O. Box 392, Colebrook, NH 03576, USA) for providing the FORTRAN code of REST2 model and Prof. Zhang Yili (Institute of Geographic Sciences and Natural Resources Research, Chinese Academy of Sciences, Beijing) for the help in data acquisition.

References

Allen R G, Trezza R, Tasumi M, 2006. Analytical integrated functions for daily solar radiation on slopes. *Agricultural and Forest Meteorology*, 139(1–2): 55–73. DOI: 10.1016/j.agrfprmet.2006.05.012

Bai Jingyu, Xu Xiangde, 2004. Atmospheric hydrological budget with its effects over tibetan plateau. *Journal of Geographical Sciences*, 14(1): 81–86. DOI: 10.1007/BF02873094

Ertekin C, Evrendilek F, 2007. Spatio-temporal modeling of global solar radiation dynamics as a function of sunshine duration for Turkey. *Agricultural and Forest Meteorology*, 145(1–2): 36–47. DOI: 10.1016/j.agrformet.2007.04.004

Gueymard C A, 2003a. Direct solar transmittance and irradiance predictions with broadband models. Part Ⅰ: Detailed theoretical performance assessment. *Solar Energy*, 74(5): 355–379. DOI: 10.1016/S0038-092X(03)00195-6

Gueymard C A, 2003b. Direct solar transmittance and irradiance predictions with broadband models. Part Ⅱ: Validation with high-quality measurements. *Solar Energy*, 74(5): 381–395. DOI: 10.1016/S0038-092X(03)00196-8

Gueymard Christian, 1989. A two-band model for the calculation of clear sky solar irradiance, illuminance, and photosyntheti-

cally active radiation at the earth's surface. *Solar Energy*, 43(5): 253–265. DOI: 10.1016/0038-092X(89)90113-8

Gueymard Christian A, 2008. REST2: High-performance solar radiation model for cloudless-sky irradiance, illuminance, and photosynthetically active radiation—Validation with a benchmark dataset. *Solar Energy*, 82(3): 272–285. DOI: 10.1016/j.solener.2007.04.008

Houborg R, Soegaard H, Emmerich W *et al*., 2007. Inferences of all-sky solar irradiance using terra and aqua MODIS satellite data. *International Journal of Remote Sensing*, 28(20): 4509–4535. DOI: 10.1080/01431160701241902

Lau K M, Kim M K, Kim K M, 2006. Asian summer monsoon anomalies induced by aerosol direct forcing: The role of the tibetan plateau. *Climate Dynamics*, 26(7–8): 855–864. DOI: 10.1007/s00382-006-0114-z

Li Chaoliu, Kang Shichang, 2006. Review of the studies on climate change since the last inter-glacial period on the Tibetan Plateau. *Journal of Geographical Sciences*, 16(3): 337–345. DOI: 10.1007/s11442-006-0309-6

Li Ren, Zhao Lin, Ding Yongjian *et al*., 2007. The features of each components in the surface heat balance equation over wudaoliang northern tibetan plateau. *Journal of Mountain Science*, 28(3): 241–247. (in Chinese)

Liu D L, Scott B J, 2001. Estimation of solar radiation in Australia from rainfall and temperature observations. *Agricultural and Forest Meteorology*, 106(1): 41–59. DOI: 10.1016/S0168-1923(00)00173-8

Mubiru J, Banda E J K B, Ujanga D F *et al*., 2007. Assessing the performance of global solar radiation empirical formulations in kampala, uganda. *Theoretical and Applied Climatology*, 87(1–4): 179–184. DOI: 10.1007/s00704-005-0196-2

Shen Zhibao, 1987. The geographic distribution of the global radiation and the characteristics of its seasonal variation over the Qinghai-Xizang Plateau. *Plateau Meteorology*, 6(4): 326–334. (in Chinese)

Stephens G L, 1978. Radiation profiles in extended water clouds. Ⅱ: parameterization schemes. *Journal of the Atmospheric Sciences*, 35(11): 2123–2132. DOI: 10.1175/1520-0469(1978)035<2123:RPIEWC>2.0.CO;2

Stephens Graeme L, Ackerman Steven, Smith Eric A, 1984. A shortwave parameterization revised to improve cloud absorption. *Journal of the Atmospheric Sciences*, 41(4): 687–690. DOI: 10.1175/1520-0469(1984)041<0687:ASPRTI>2.0.CO;2

Van Laake P, Sanchez-Azofeifa G A, 2004. Simplified atmospheric radiative transfer modelling for estimating incident par using modis atmosphere products. *Remote Sensing of Environment*, 91(1): 98–113. DOI: 10.1016/j.rse.2004.03.002

Wang Quan, Tenhunen John, Schmidt Markus *et al*., 2006. Estimation of total, direct and diffuse par under clear skies in complex alpine terrain of the national park Berchtesgaden, Germany. *Ecological Modelling*, 196(1–2): 149–162. DOI: 10.1016/j.ecolmodel.2006.02.005

Winslow J C, Hunt E R, Piper S C, 2001. A globally applicable model of daily solar irradiance estimated from air temperature and precipitation data. *Ecological Modelling*, 143(3): 227–243. DOI: 10.1016/S0304-3800(01)00341-6

Wu Guoxiong, Liu Yimin, Liu Xin *et al*., 2005. How the heating over the Tibetan Plateau affects the asian climate in summer. *Chinese Journal of Atmospheric Science*, 29(1): 47–56. (in Chinese)

Wyser K, O Hirok W, Gautier C *et al*., 2002. Remote sensing of surface solar irradiance with corrections for 3-D cloud effects. *Remote Sensing of Environment*, 80(2): 272–284. DOI: 10.1117/12.373064

Xu Weixin, Liu Xiaodong, 2007. Response of vegetation in the Qinghai-Tibet Plateau to global warming. *Chinese Geographical Science*, 17(2): 151–159. DOI: 10.1007/s11769-007-0151-5

Yang K, Huang G W, Tamai N, 2001. A hybrid model for estimating global solar radiation. *Solar Energy*, 70(1): 13–22. DOI: 10.1016/S0038-092X(00)00121-3

Yang K, Koike T, Ye B S, 2006. Improving estimation of hourly, daily, and monthly solar radiation by importing global data sets. *Agricultural and Forest Meteorology*, 137(1–2): 43–55. DOI: 10.1016/j.agrformet.2006.02.001

Zelenka A, Perez R, Seals R *et al*., 1999. Effective accuracy of satellite-derived hourly irradiances. *Theoretical and Applied Climatology*, 62(3–4): 199–207. DOI: 10.1007/s007040050084

Zhang Yili, Li Bingyuan, Zheng Du, 2002. A discussion on the boundary and area of the Tibetan Plateau in China. *Geographical Research*, 21(1): 1–8. (in Chinese)